Iraqi National Journal of Chemistry

Journal homepage:
http://iqnjc.com/Default.aspx

Molecular charge distributions, Vibrational frequency and Stability studies on 1H-indole-3-carbaldehyde and (Z)-indol-3-ylidenemethanol: DFT Approach

IBRAHIM Omotayo Asiata, OYEBAMIJI Abel Kolawole and SEMIRE Banjo*

Department of Pure and Applied Chemistry, Faculty of Pure and Applied Sciences, Ladoke Akintola University of Technology, Ogbomoso, Nigeria

*Corresponding e-mail: bsemire@lautech.edu.ng

Abstract

1H-indole-3-carbaldehyde (A) and its enol-tautomer, (Z)-indol-3-ylidenemethanol (B) have been examined using B3LYP/6-311++G(d,p), M06/6-311++G(d,p), wB97xD/6-311++G(d,p) and MP2/6-311++G(d,p) methods. The E_{HOMO}, E_{LUMO}, $\Delta(E_{HOMO-LUMO})$, dipole moment, softness (σ), chemical hardness (η), chemical potential (μ), ionization potential (IP), electron affinity (EA), nucleophilicity index (ω) and thermodynamic parameters were calculated and discussed. The band gap revealed that compound A would be hard, more stable thermodynamically and less labile than B. This this was in agreement with the total energy, chemical hardness and chemical softness calculated for the compounds. The Molecular electrostatic potential (MEP) map showed that N-H hydrogen and carbonyl oxygen are the most plausible potential site for nucleophilic (blue color) and electrophilic (red color) activities for compound A. For compound B, O-H hydrogen and N of indole are most plausible site for nucleophilic and electrophilic activities. Critical analysis of the charge population distributions shows that charge distributions respond more to the basis sets rather than the computational methods used for the calculations.

Keywords: 1H-indole-3-carbaldehyde, (Z)-indol-3-ylidenemethanol, Molecular Properties, DFT

1.0 Introduction

Indole and its derivatives are present naturally in both animals and plants, such as tryptophan in human and in plant as alkaloids like serotonin and tryptamin [1,2]. They are important classes of compounds used in medicinal chemistry as therapeutical agents such as anti-cancer [3], antirheumatoidal [4] and anti-HIV [5] as well as antioxidant [6]. Indole-2-carboxylic acid hydrochloride is one of the noticeable indole derivatives that possesses various important biological activities as such as antihypertensive [7]; antiarrhytmic [8], anticonvulsant effects [9] and antifungal [10,11] properties. The biological activity of the indole derivatives is attributed to the nature of substituent in position 3 on the pyrrole ring. Several highly selective drugs contain indole structure are commercially available such as Sumatriptan, Ondansetron, Arbidol, Roxindole, Pindolol, Trandolapril and Perindopril [12-14].

In addition, due to the importance of indole derivatives afore-mentioned above, several indole derivative have been synthesized and structurally elucidated in last sixty years [15-19]. Theoretically, various quantum chemical methods have been used to study indole derivatives such as semi-empirical [20], ab initio [21, 22], density functional theory (DFT) for the frequency calculations of the indole molecule [23-28]. Recently, indole and its derivatives namely; 1H-indole-3-carbaldehyde (3-formylinodole), 1-methyl-3-formylindole, 1-ethyl-3-formylindole, 3-acetylindole, 1-methyl-3-acetylindole, 1-ethyl-3-acetylindole and 1,3-diacetylindole have been studied both experimentally and theoretically to throw light on the effect of substituents on indole. The results showed that substitution caused minor changes in the molecular geometry, but substantially altered the charge distributions and vibrational force constants of the studied indole derivatives compared to indole. Also, it was shown that the alkyl substitution shifted the aldehyde carbonyl stretch band frequencies to higher frequency values [29].

However, in this present study, 1H-indole-3-carbaldehyde (3-formylindole) and its enol-tautomer ((Z)-indol-3-ylidenemethanol) are examined by quantum chemical calculations using Density Functional theory (DFT) and Mϕller Plesset (MP2) methods with various basis sets. The enol-tautomer of the 3-formylindole has not been synthesized neither discussed in the literature to the best of our knowledge. Therefore, this paper would focus mainly on; (i) quantum chemical calculations on stability and reactivity study of 3-formylindole and its enol-tautomer, (ii) comparison of theoretical results on 3-formylindole with the experimental data available in the literature, and (iii) comparison of theoretical results on 3-formylindole with its enol-tautomer ((Z)-indol-3-ylidenemethanol) as shown in Figure 1.

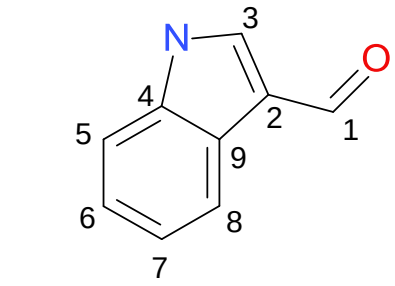

(Ai)

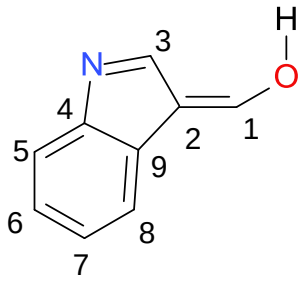

(Bi)

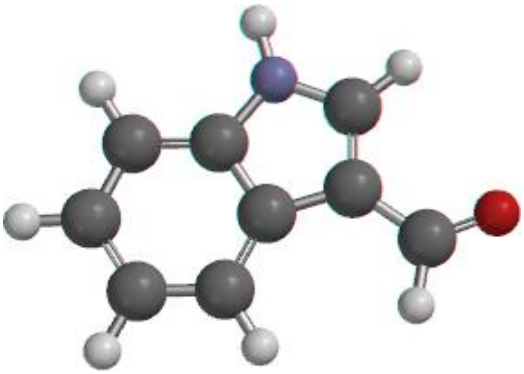

(Aii)

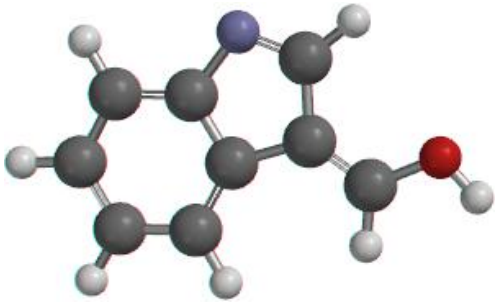

(Bii)

Figure 1: Schematic and Optimized structures of the studied molecules with numbering of atoms: (a) 1H-indole-3-carbaldehyde (3-formylindole) and (b) (Z)-indol-3-ylidenemethanol

2.0 Computational details

Conformation search was performed on each of the compound using semi-empirical (AM1) method with Monte Carlo search algorithm to identify the most stable conformer. The lowest-energy conformer in each conformational search was selected for geometry optimization at density functional theory (DFT) levels of theory. Therefore, the geometry optimization was carried out on the most stable conformer with Beckes's three-parameter hybrid functional [30] employing the Lee, Yang and Parr correlation functional B3LYP [31]. Furthermore, the optimized structure from B3LYP/6-311++G(d,p) calculations was used as a starting structure for geometrical optimization at M06/6-311++G(d,p), wB97xD/6-311++G(d,p) and MP2/6-311++G(d,p) levels. The vibration frequency and energy calculations were performed on the optimized geometry at B3LYP/6-311++G(d,p) and wB97xD/6-311++G(d,p) respectively. Also, the absorption transitions were calculated at TD-B3LYP/6-311++G(d,p) and TD-wB97xD/6-311++G(d,p) levels on the optimized geometry. However, the convergence criteria used for the geometry optimizations and energy calculations in the present study were default parameters as implemented in the Spartan 14 program [32]. The molecular parameters calculated using DFT/6-311++G (d,p) were energy of the highest molecular orbital (EHOMO), energy of lowest

unoccupied molecular orbital (ELUMO), dipole moment, energy gap electronegativity, chemical hardness, softness, nucleophilicity, chemical potential and electron affinity.

Conceptual DFT was used for the calculations of global descriptors, according to Koopman's theorem global hardness, softness, electronegativity, chemical potential and electronegativity are defined in terms of energy of LUMO and HOMO [33-36] for calculating the global descriptors;

(i) Chemical hardness

$$\eta = \frac{IP+EA}{2} = \frac{E_{HOMO}+E_{LUMO}}{2}$$

where IP = ionization potential and EA = electron affinity.

(ii) Chemical softness (s): This determines the reactivity of the molecule and it is calculated using the formula; $(s) = \frac{1}{2\eta}$

(iii) Electronegativity

$$\mu = \frac{dE}{dN}V(r) = -\chi = -\frac{IP+EA}{2} = \frac{E_{HOMO}+E_{LUMO}}{2}$$

where E is the total energy of the molecule, N is number of electrons and v(r): external potential of the system.

(iv) Global electropilicity/ nucleopilicity index, $\omega = \frac{\mu^2}{2\eta}$

3.0 Results and discussion

3.1 Stability and Geometrical properties

The total energies of 1H-indole-3-carbaldehyde (A) and (Z)-indol-3-ylidenemethanol (B) calculated using different quantum chemical methods are displayed in Table 1. These energies for compounds A and B are -4.77.27 and -477.25 au for B3LYP/6-311++G(d,p), -4.77.12 and -477.07 au for wB97xD/6-311++G(d,p), -476. 93 and -476.90 au for MO6/6-311++G(d,p) and -475.91 and -475.88 au for MP2/6-311++G(d,p). This indicates that compound A is more stable

by 18.60, 28.43, 19.36 and 19.13 kcal/mol as calculated by B3LYP/6-311++G(d,p), wB97xD/6-311++G(d,p), MO6/6-311++G(d,p) and MP2/6-311++G(d,p) respectively; thus showing that the stability predicted by B3LYP, MO6 and MP2 are quantitatively the same (≈ 19.0 kcal/mol).

Furthermore, the geometrical parameters for compounds A and B calculated using B3LYP, wB97xD, MO6 and MP2 methods with 6-311++G(d,p) basis set as well as the selected experimental geometrical parameters for compound A are listed in Table 1. The geometrical parameters calculated using various computational chemistry methods show good approximation, and they can be used to calculate/predict geometries of similar compounds with reasonably high accuracy, although that of MP2 is relatively closer the experimental data (Figure 2). Therefore, the geometrical parameters calculated for compound B at MP2/6-311++G(d,p) can be used to work with in the absence of experimental data. Generally, calculated bond lengths are slightly longer than X-ray values, this is due to the fact that experimental result corresponds to interacting molecules in the crystal lattice, meanwhile computational method deals with an isolated molecule in gaseous phase [38,39] as well as level of computational method in use [40]. For instance, the N-C3 (N-C4) bond lengths for compound A are 1.364 (1.389), 1.359 (1.384), 1.362 (1.386) and 1,342 (1.382 Å) as calculated by B3LYP/6-11++G(d,p), wB97xD/6-11++G(d,p) MO6/6-11++G(d,p) and MP2/6-11++G(d,p) respectively. These bond lengths were experimentally observed at 1.334 and 1.380 for N-C3 and N-C4 respectively [37]. However, for compound B, these bond lengths are calculated at B3LYP/6-11++G(d,p), wB97xD/6-11++G(d,p) MO6/6-11++G(d,p) and MP2/6-11++G(d,p) to be 1.287 (1.414), 1.289 (1.413), 1.294 (1.415) and 1,250 (1.411 Å) respectively. This shows that N-C3 and N-C4 bond lengths are shorter than usual N-C single bond due to delocalization of lone pair of electron on nitrogen atom in the ring of compound A, whereas in compound B, N-C3 and N-C4 display typical double and single bond lengths characters respectively. Also, the C1-O (C1-C2) bond lengths are calculated to be 1.218 (1.455), 1.211 (1.455), 1.215 (1.454) and 1.216 (1.432Å) at B3LYP/6-11++G(d,p), wB97xD/6-11++G(d,p) MO6/6-11++G(d,p) and MP2/6-11++G(d,p) respectively; these are experimentally obtained at 1.218 and 1.422Å for C1-O and C1-C2 respectively. For compound B, the C1-O (C1-C2) bond lengths are 1.352 (1.346), 1.343 (1.339), 1.348 (1.341) and 1.350 (1.338Å) at B3LYP/6-11++G(d,p), wB97xD/6-11++G(d,p) MO6/6-11++G(d,p) and MP2/6-11++G(d,p) levels respectively. Figure 2 shows the performance of the theoretical methods used in predicting/calculating the bond lengths of compound A compared to the experimental values.

The bond angels calculated for compound A are generally closer to the experimental than the bond lengths. The OC1C2 (NC4C5) bond angles in the X-ray structure of compound A are 125.4° (129.30°), whereas these are calculated to be 124.99 (130.12), 124.76 (129.97), 125.01 (130.00) and 125.35°(129.18°) at B3LYP/6-11++G(d,p), wB97xD/6-11++G(d,p) MO6/6-11++G(d,p) and MP2/6-11++G(d,p) levels respectively. For compound B, these bond angles are 122.11 (127.02), 122.21 (126.81), 122.19 (127.22) and 122.15°(112.78°) as calculated by B3LYP/6-11++G(d,p), wB97xD/6-11++G(d,p) MO6/6-11++G(d,p) and MP2/6-11++G(d,p) respectively. Similarly, the bond angle at the nitrogen (C3NC4) in the X-ray of compound A is 109.04° [37], this bond angle is 109.88, 109.70, 109.28 and 108.01°; however, it is calculated to

be 106.50, 106.47, 106.35 and 106.40° for compound B at B3LYP/6-11++G(d,p), wB97xD/6-11++G(d,p) MO6/6-11++G(d,p) and MP2/6-11++G(d,p) respectively, which shows that compound B experienced more strain around nitrogen atom in the indole ring (Table 1).

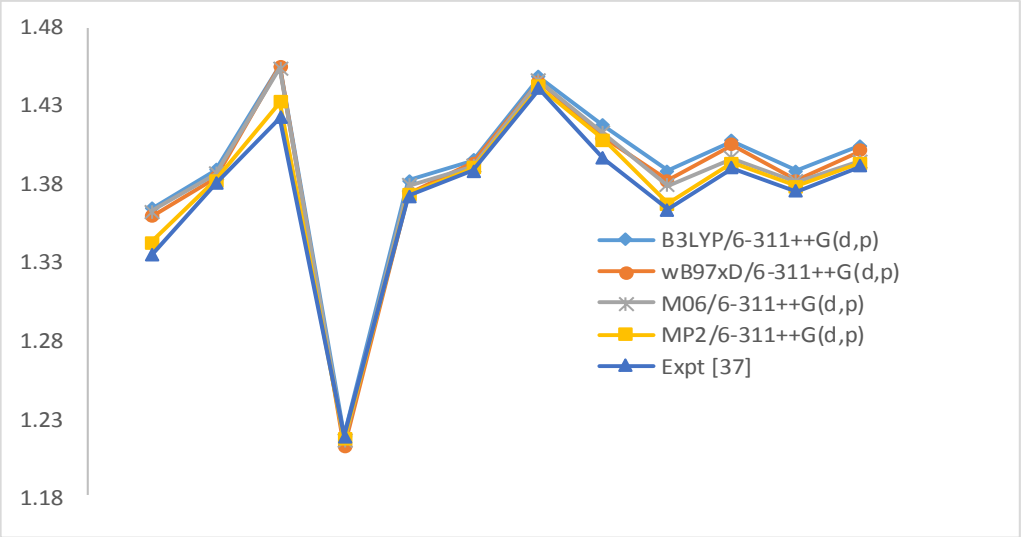

Figure 2: comparison of calculated and experimental bond lengths

Table 1: Total energies and selected geometries for the tautomers; bond distances (Å) and bond angles (°)

	A					B			
	B3LYP/6-311++G(d,p)	wB97xD/6-311++G(d,p)	M06/6-311++G(d,p)	MP2/6-311++G(d,p)	Expt [37]	B3LYP/6-311++G(d,p)	wB97xD/6-311++G(d,p)	M06/6-311++G(d,p)	MP2/6-311++G(d,p)
E_{Total} (au)	-477.274856	-477.117176	-476.928922	-475.910970	-	-477.245215	-477.071866	-476.898077	-475.880491
N-C3	1.364	1.359	1.362	1.342	1.334(3)	1.297	1.289	1.294	1.285
N-C4	1.389	1.384	1.386	1.382	1.380 (3)	1.414	1.413	1.415	1.411
C1-C2	1.455	1.455	1.454	1.432	1.422 (3)	1.346	1.339	1.341	1.338
C1-O	1.218	1.211	1.215	1.216	1.218 (2)	1.352	1.343	1.348	1.350
C2-C3	1.382	1.374	1.379	1.373	1.372 (3)	1.468	1.467	1.465	1.458
C4-C5	1.395	1.393	1.391	1.390	1.388 (3)	1.389	1.386	1.387	1.385
C2-C9	1.448	1.445	1.446	1.442	1.441 (3)	1.466	1.464	1.463	1.462
C4-C9	1.417	1.409	1.412	1.408	1.396 (3)	1.413	1.405	1.410	1.409
C5-C6	1.388	1.382	1.379	1.367	1.363 (3)	1.397	1.392	1.395	1.394
C6-C7	1.407	1.405	1.396	1.393	1.390 (3)	1.399	1.396	1.395	1.391
C7-C8	1.388	1.382	1.381	1.378	1.375 (3)	1.398	1.392	1.395	1.388
C8-C9	1.404	1.401	1.394	1.393	1.391 (3)	1.391	1.387	1.388	1.385
OC1C2	124.99	124.76	125.01	125.35	125.4 (2)	122.11	122.21	122.19	122.15
C3C2C1	124.93	124.96	124.03	124.01	123.8 (2)	127.95	128.00	127.85	127.64
C3C2C9	106.72	106.71	106.44	106.40	105.93 (19)	103.78	103.67	103.78	103.38
C1C2C9	128.35	128.33	129.88	130.35	130.22 (19)	128.26	128.29	128.88	128.02
NC3C2	109.57	109.65	109.97	110.60	110.8 (2)	113.21	113.30	113.24	112.78
NC4C5	130.12	129.97	130.00	129.18	129.30 (19)	127.02	126.81	127.22	126.98
NC4C9	107.13	107.32	107.62	107.73	107.95 (18)	111.73	111.93	111.70	111.65
C5C4C9	122.75	122.71	122.55	122.68	122.65(19)	121.25	121.26	121.22	121.20
C6C5C4	117.27	117.23	117.06	117.20	117.2(2)	118.07	117.99	118.10	118.07
C5C6C7	121.07	121.12	121.36	121.37	121.4 (2)	120.96	120.99	120.96	120.94
C8C7C6	121.32	121.28	121.33	121.41	121.4 (2)	120.96	120.95	120.94	120.92

C7C8C9	118.92	118.84	118.42	118.45	118.5 (2)	118.43	118.30	118.38	118.39
C8C9C4	118.65	118.81	118.95	118.85	118.84 (19)	120.34	120.52	120.30	120.26
C8C9C2	134.64	134.57	134.68	134.69	134.75 (18)	134.98	134.85	134.96	134.95
C4C9C2	106.70	106.62	106.40	106.28	106.31 (17)	104.68	104.63	104.58	104.55
C3NC4	109.88	109.70	109.28	109.01	109.04(16)	106.50	106.47	106.35	106.40

3.2 Vibrational frequencies (cm^{-1})

The use of spectroscopic techniques particularly vibrational spectroscopy has been widely acceptable method for the elucidation of the structures of organic compounds. This method is very especial for functional groups, conformers, tautiomers and isomers identifications [41]. Critical analysis of the experimental and theoretical vibration modes is very helpful in understanding the functional groups of a fairly complex system. However, where experimental data are not available, theoretical simulated vibrational frequencies have been found to have reasonable degree of accuracy [39,40, 42], which can be useful in understanding the properties of a molecule as well as effect of functional groups on the molecules. The accuracy of the calculated vibrational frequencies can be improved by scaling. The scale factors recommended for better accurate prediction for IR frequencies calculated are 0.8953, 0.9682 and 0.9668 at HF/6-31G*, B3LYP/6-31G* and B3LYP/6-311++G** respectively [43-45]. Although, the vibrational frequencies presented in this work were scaled by 0.96 [46, 47] and compared to the skeletal experimental data available, especially for compound A [29,48]. The calculated IR values and simulated spectra are shown in Table 2 and Figure 3 respectively.

The N-H stretching vibrations for compound A were reported at 3484 cm^{-1} [48] and 3443.7 [29], but calculated at 3652 cm^{-1} and scaled down to 3505 cm^{-1}. This is similar to vN-H observed for Indole-2-carboxylic acid (ICA) at 3350 cm^{-1} which was assigned to the intermolecular N–H· · ·O hydrogen bond. But, it was observed at 3453 cm^{-1} which was non-associated N–H groups in the ICA crystal [49]. However, the calculated vO-H vibrations for compound B was at 3853 cm^{-1} and scaled to 3699 cm^{-1}. The pure πOH vibrations for B was predicted at 1282, although the impure coupled other vibrations was theoretically observed at 1331 cm^{-1} (vC2-C9 + πC-H ph + πO-H), 1182 cm^{-1} (πC-H ph + πO-H) and 1168 cm^{-1} (πC-H ph + πC3-H + πO-H). The pure σOH vibrations for B was predicted at 392, 294 and 260 cm^{-1}.

The vC-H band aromatic for compound A was reported at 3055 cm^{-1} [48] or 3068.3, 3063.3 and 3045.4 cm^{-1} [29], this was calculated to be between 3195 and 3168 cm^{-1}. For compound B, it was between 3185 and 3155 cm^{-1}. The vC3-H vibrations was reported at 3164 [48] and 3115.3 [29], but was calculated at 3261 and 3198 cm^{-1} for A and B respectively. The vC1-H vibrations (i.e. carbonyl hydrogen) was at 2813 and 2821.9 cm^{-1} [29, 48] for compound A, this was calculated at 2903 and 3152 cm^{-1} for A and B respectively. The C–H in-plane bending vibrations (πCH) theoretically calculated were in-pure in the gas phase. The πCH vibrations were calculated in the region 1347-1147 cm^{-1} and 1037-1498 cm^{-1} for A and B respectively, these were observed the region 1009-1383 cm^{-1} for compound A [48]. The πC3-H vibrations were 1114 and 1304 cm^{-1} for compounds A and B respectively. For the C–H out-of-plane bending (σCH) vibrations, this was observed at 792 cm^{-1} for compound A; however it was theoretically predicted at 1016, 981, 853 and 748 cm^{-1} for compound A, and 978, 945, 866, 773 and 750 cm^{-1} for compound B. The σC3-H vibrations were 853 cm^{-1} for A, and 903 and 650 cm^{-1} B.

Table 2: Vibrational frequencies calculated at B3LYP/6-311++G(d,p) method

Compound A				*Compound B*		
Expt [29*,48]	Cal.	Scaled	Assign.	Theor.	Inten.	Assign
3484 (3443.7)*	3652	3505.92	vN-H	3853	3698.88	vO-H
3164 (3115.3)*	3261	3130.56	vC3-H	3198	3070.08	vC3-H
3055 (3068.3, 3063.3, 3045.4)*	3195	3067.20	Syn vC-H ph	3196	3068.16	Syn vC-H Ph
	3185	3057.6	antsy vC-H ph	3185	3057.6	Ant vC-H Ph
	3175	3048	antsy vC-H ph	3170	3043.2	Syn vC-H Ph
	3168	3041.28	antsy vC-H ph	3155	3028.8	vC-H Ph + vC1-H
2813 (2821.9)*	2903	2786.88	vC1-H	3152	3025.92	vC1-H
1635 (1633.4)*	1733	1663.68	vC=O	1722	1653.12	vC1=C2
1522	1657	1590.72	vC=C ph	1647	1581.12	vC=C ph
	1614	1549.44	vC=C ph	1618	1553.28	vC=C ph
	1553	1490.88	vC2=C3	1550	1488	vC=N
	1523	1462.08	v(C=C ph + C-N)	1498	1438.08	v(C=C) ph + πC-H
	1480	1420.8	C=C ph + πC-H	1472	1413.12	vC=C ph + πC-H
	1460	1401.6	vC-N + πN-H + πC1-H	1410	1353.6	vC1=C2 + πC1-H
1383	1421	1364.16	vC-N + πN-H + πC1-H	1373	1318.08	vC=C ph + πC-H
	1368	1313.28	vC=C ph	1331	1277.76	vC2-C9 + πC-H ph + πO-H
	1347	1293.12	vC=C ph + πC-H	1304	1251.84	πC3-H
1383	1332	1278.72	vC1-C2 + πC3-H + πC1-H	1282	1230.72	πO-H
	1261	1210.56	vC2=C3 + πC-H	1235	1185.6	vC1-O
	1250	1200	vC-N + πN-H	1188	1140.48	vC-N + πC-H
	1179	1131.84	πC-H ph	1182	1134.72	πC-H ph + πO-H
	1150	1104	πC-H ph + πC3-H	1168	1121.28	πC-H ph + πC3-H + πO-H
1009	1114	1069.44	πC3-H	1114	1069.44	πC-H ph
	1069	1026.24	vC2-C1	1052	1009.92	
	1034	992.64	Ring breathing	1033	991.68	πC-H ph
	1016	975.36	σC1-H	978	938.88	σC-H ph
	981	941.76	σC-H ph	945	907.2	σC-H ph
	940	902.4	σC-H ph	919	882.24	σC2-H + σC3-H
877	887	851.52	Ring rocking	903	866.88	σC3-H
792	855	820.8	σC-H ph + σC3-H	876	840.96	Rocking ring

	853	818.88	σC3-H	866	831.36	σC-H ph
	827	793.92	Ring breathing	796	764.16	Ring breading
	771	740.16	σRing	773	742.08	σC-H ph
740	754	723.84	Ring breathing	750	720	σC-H ph
	748	718.08	σC-H ph	735	705.6	Ring breading
	654	627.84	Ring rocking	650	624	σC3-H
	626	600.96	σN-H + σC3-H	641	615.36	Rocking ring
	583	559.68		580	556.8	
526	565	542.4	Ring breathing	570	547.2	Rocking ring
	478	458.88	Ring breathing	491	471.36	Rocking ring
	478	458.88	σC-H	440	422.4	
	425	408		392	376.32	σO-H
	355	340.8	Ring rocking	343	329.28	
	304	291.84		294	282.24	σO-H
	226	216.96	σRing	260	249.6	σO-H
	179	171.84	σC1-H	185	177.6	σ(C1-O-H)
	154	147.84		152	145.92	
	98	94.08		93	89.28	

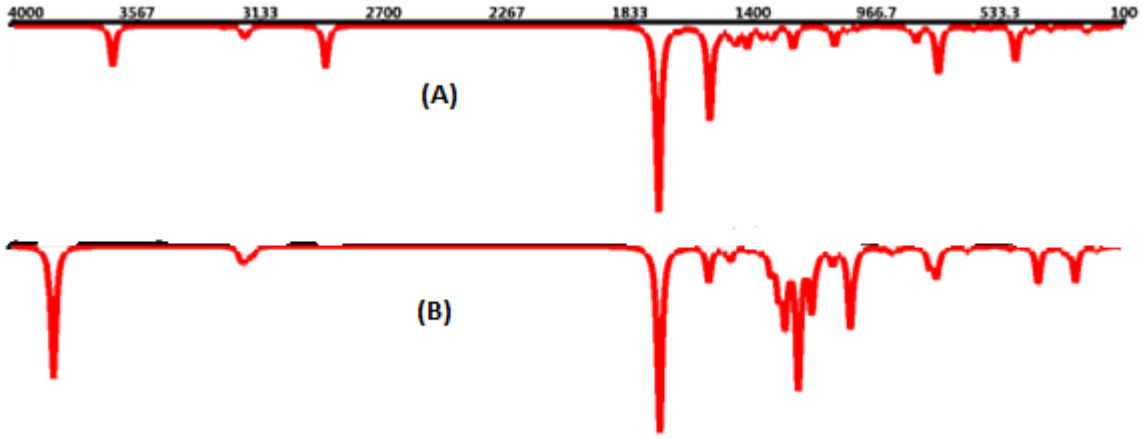

Figure 3. Simulated IR spectra for compounds A and B at B3LYP/6-311++G(d,p).

3.3 Global reactivity and Electronic properties

The highest occupied molecular orbital energy (E_{HOMO}), lowest unoccupied molecular orbital energy (E_{LUMO}), $\Delta(E_{HOMO-LUMO})$, dipole moment, softness (σ), chemical hardness (η), chemical potential (μ), ionization potential (IP), electron affinity (EA), nucleophilicity index (ω) and thermodynamic parameters calculated using B3LYP/6-311++G(d,p) and MO6/6-311++G(d,p) methods are displaced in Tables 3. The HOMO and LUMO symbolize the electron donating and accepting abilities of a molecule respectively. The E_{HOMO}, E_{LUMO} and energy gap are calculated to be -6.33, -1.64 and 4.69 eV, and -6.62, -1.49 and 5.13 eV at B3LYP/6-311++G(d,p) and MO6/6-311++G(d,p) respectively for compound A. These parameters are -6.36, -2.13 and 4.23 eV, and -6.63, -1.98 and 4.65 eV as calculated by B3LYP/6-311++G(d,p) and MO6/6-311++G(d,p) respectively for compound B. Both

DFT and MO6 methods predicted the HOMO energy of compound A to be higher than B, indicating that compound A would donate electrons to a poor electrons specie readily then B. Meanwhile, the LUMO energy of B is calculated to be lower than A thus readily accept electrons form electron donor compound. The energy gap calculated reveals that compound A would be hard, more stable thermodynamically and less labile than B, this is in agreement with the total energy, chemical hardness and chemical softness calculated for the compounds (Table 1). The frontier molecular orbital maps i.e. the HOMO-2, HOMO-1, HOMO, LUMO and LUMO+1 for compounds A and B are displayed in Figure 4.

Moreover, the IP values for A and B are 6.33 and 6.36 eV as calculated by DFT , and calculated to be 6.62 and 6.63 eV by MO6 method. This shows that compound A has lower energy ionization, enhance lower energy is required for the electron to be removed from the HOMO orbital. The EA on the other hand reveals that compound B is capable accepting electron readily than compound B. The μ and ω values are -3.985 and 3.386 eV for A, and -4.245 and 4.260 eV for B respectively. These are also indications that A would be a better nucleophile than B.

Another significant electronic parameter to predict the interaction of a compound with solvent is dipole moment which results from non-uniform distribution of charges on the various atoms in the molecule. The orientation of the electric dipole moment vector (m) determines electrochemical characteristics of a molecule, and also, the structure of the electrical double layer at the surface of electrodes which governs the kinetics of the diffusion-controlled electrode reactions depends on the dipole moment of the solute molecules [50, 51]. Thus, the calculated values of dipole moment for compound A and B show that B would have stronger intersections with solvents especially polar ones. The calculated standard enthalpy *(kJ mol^{-1})*, entropy *(J mol^{-1} K^{-1})* and Gibb's free energy *(kJ mol^{-1})* calculated at 298 K and 1 atm using B3LYP/6-311++G(d,p) method are 386.734, 365.633 and 277.723 for A, and 386.306, 366.165 and 277.134 for B respectively.

Table 3. Molecular properties of compounds A and B calculated at B3LYP/6-311++G(d,p) and M06/6-311++G(d,p) methods

Property	*A*		*B*	
	B3LYP/6-311++G(d,p)	M06/6-311++G(d,p)	B3LYP/6-311++G(d,p)	M06/6-311++G(d,p)
E_{HOMO} (eV)	-6.33	-6.62	-6.36	-6.63
E_{LUMO} (eV)	-1.64	-1.49	-2.13	-1.98
Energy gap (H-L) eV	4.69	5.13	4.23	4.65
Ionization potential (IP)	6.33	6.62	6.36	6.63
Electron affinity (EA)	1.64	1.49	2,13	1.98
Chemical hardness η	2.345	2.565	2.115	2.325
Chemical softness (σ) eV^{-1}	0.213	0.195	0.236	0.215
Chemical potential (μ)	-3.985	-4.055	-4.245	-4.305
Electronegativity (χ)	3.985	4.055	4.245	4.305
Global electrophilicity (ω)	3.386	3.205	4.260	3.986
Dipole moment (Debye)	4.62	4.57	5.22	5.21
Standard Enthalpy (kJ mol^{-1})	386.7368		386.3063	
Standard Entropy (J mol^{-1} K^{-1})	365.6331		366.1653	
Standard Free energy (kJ mol^{-1})	277.7233		277.1341	

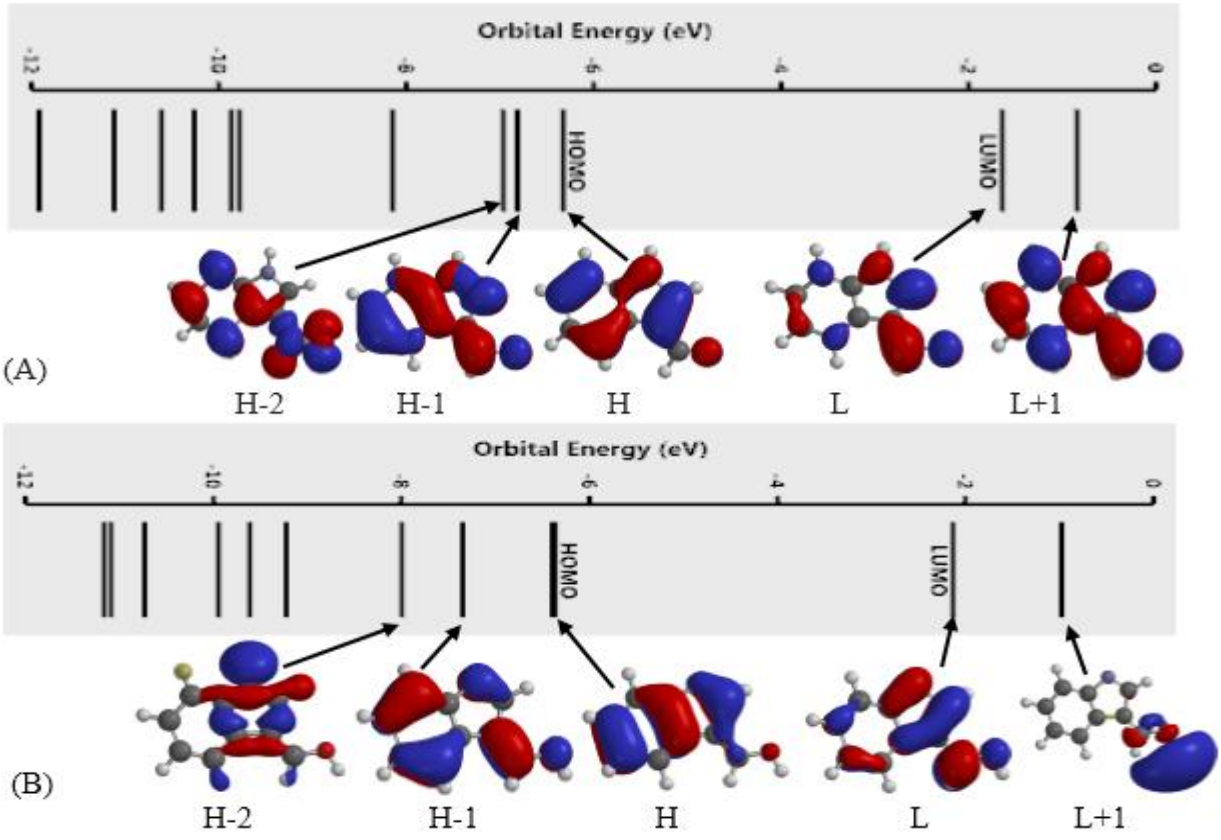

Figure 4: The frontier orbitals energies for compounds A and B at B3LYP/6-311++G(d,p) level.

The absorption peaks, oscillator strength (*f*) and molecular orbital component involved in transitions for A and B as calculated by wB97xD/6-311++G(d,p) and B3LYP/6-311++G(d,p) are listed in Table 4. The transitions arising from low absorption bands oscillator strength (*f*) values less than 0.005 are not discussed in this paper. The calculated absorption transitions at wB97xD/6-311++G(d,p) for compound A has four strong absorption (i.e. > 0.005 *f*) at 210.58, 225.30, 240.71 and 245.74 nm with 0.1721, 0.1094, 0.1073 and 0.1502 *f* respectively. These absorption bands are calculated at B3LYP/6-311++G(d,p) to be 238.37, 247.20, 269.42 and 275.22 nm with 0.0511, 0.0779, 0.0207 and 0.1551 *f* respectively. The 221.50 nm absorption peak arises from the HOMO-1 → LUMO+3 (0.43), HOMO → LUMO+3 (0.22), HOMO-3→ LUMO (0.14), HOMO → LUMO (0.12) which is characterized as π-π* and n-π* transitions as predicted by wB97xD/6-311++G(d,p) calculations. However, the λmax (275.22 nm) arises from the HOMO → LUMO (0.82) is characterized as π-π* transition as predicted by B3LYP/6-311++G(d,p).

Furthermore, for compound B, the calculated absorption transitions at wB97xD/6-311++G(d,p) also has four strong absorption bands (i.e. > 0.005 *f*) at 209.58, 221.50, 274.10 and 2294.33 nm with 0.0781, 0.6599, 0.2383 and 0.0302 *f* respectively. For B3LYP/6-311++G(d,p) calculations, three strong absorption bands (i.e. > 0.005 *f*) are observed at 231.50, 301.14 and 343.11nm with 0.2458, 0.1769 and 0.0243 *f* respectively. The 210.58 nm absorption peak arises from the HOMO-1 → LUMO+2 (0.40), HOMO-1→ LUMO (0.34), HOMO→ LUMO+2 (0.13) is characterized as π-π* and n-π* transitions as predicted by wB97xD/6-311++G(d,p) calculations. However, the λmax (301.14 nm) arises from the HOMO → LUMO (0.69) is characterized as π-π* transition as predicted by B3LYP/6-311++G(d,p). The two DFT methods used for the calculations of adsorption bands show that compound B presented a longer absorption wavelength than compound A, this is in agreement with energy band gap and IP as shown in Tables 3 and 4.

Table 4: Absorption peaks, oscillation strengths, and molecular orbitals (MOs) involved in transitions for compounds A and B.

	A			B		
	UV	*f*	MO	*UV*	*f*	MO
wB97xD/6-311++G(d,p)	210.58 212.15 225.30 240.71 245.74	0.1721 0.0017 0.1094 0.1073 0.1502	H-1 -> L+2 (0.40), H-1 -> L (0.34), H -> L+2 (0.13) H -> L+1 (0.88) H -> L+2 (0.73) H-1 -> L (0.51), H -> L+6 (0.18), H -> L (0.11) H -> L (0.77)	209.58 221.50 268.98 274.10 294.33	0.0781 0.6599 0.2383 0.0028 0.0302	H -> L+3 (0.57), H-1 -> L+3 (0.22) H-1 -> L+3 (0.30), H -> L+3 (0.22), H-3 -> L (0.14), H -> L (0.12) H -> L (0.74) H-2 -> L (0.94) H-1 -> L (0.87)
B3LYP/6-311++G(d,p)	238.37 247.20 269.42 275.22	0.0511 0.0779 0.0207 0.1551	H-1-> L+1 (0.52), H -> L+1 (0.17), H -> L+4 (0.14) H -> L+1 (0.58), H -> L+4 (0.19), H-1 -> L+1 (0.12) H-1 -> L (0.75) H -> L (0.82)	231.50 301.14 304.86 343.11	0.2458 0.1769 0.0020 0.0243	H -> L+2 (0.40), H-1 -> L+2 (0.33), H-1 -> L+5 (0.14) H-1 -> L (0.68) H-2 -> L (0.99) H -> L (0.87)

3.4. Molecular electrostatic potential (MEP)

The electrostatic potential V(r) shows static distributions of charge on a molecule. This has been a very useful property for analyzing and predicting molecular reactive behavior to indicate sites or regions of a molecule where an approaching electrophile/nucleophile is initially attracted [52, 53, 54]. The differences of the electrostatic potential at the surface are represented by different colors. The negative regions (red, orange and yellow color) of MEP with the high electron density are associated to electrophilic reactivity, the positive regions (blue color) with the low electron density ones to nucleophilic reactivity and the green color is neutral regions. The MEP of the compounds A and B calculated at B3LYP/6-311++G(d,p) level of energy is shown in Figure 5. The negative (red color) and positive (blue color) regions of the compound A are mainly on carbonyl oxygen atom and N-H hydrogen with surface potential of -202.38 and 283.23 kJ/mol respectively. Meanwhile, for compound B, the negative (red color) and positive (blue color) regions are mainly on Nitrogen atom of indole and O-H hydrogen with surface potential of -210.54 and 337.33 kJ/mol respectively. According to MEP map, N-H hydrogen is the most plausible potential site for nucleophilic activity (blue color) and carbonyl oxygen is the most suitable site for electrophilic activity (red color) for compound A. However, for compound B, O-H hydrogen is the most plausible site for nucleophilic activity

(blue color) and N atom of indole is the most feasible potential site for electrophilic activity (red color).

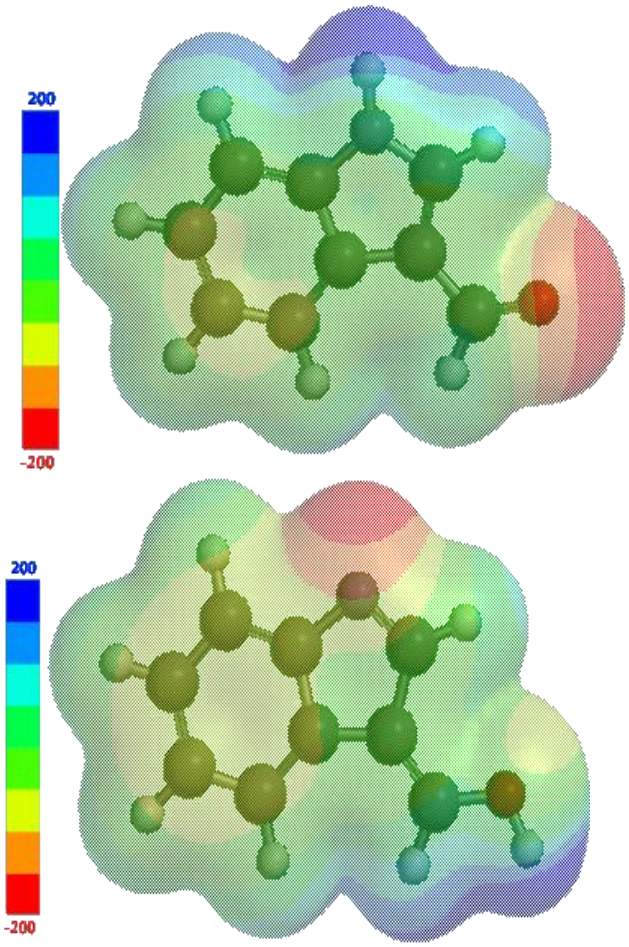

A B

Figure 5: Molecular electrostatic potential (MEP) map of compounds A and B calculated at B3LYP/6-311++G(d,p) level.

3.5 *The effects of computational methods on electronic charges*

The compounds A and B were optimized with different computational methods such as B3LYP, wB97xD, MO6 and MP2 with 6-311++G(d,p) basis set, and electronic charges (electron densities) calculated based on these methods were examined. Calculations of electron densities are important in rationalizing chemical reactions, and also, for physico-chemical properties of molecules, because charge-based parameters are mostly used as chemical reactivity indices or to measure weak intermolecular interactions. Although, the most popular methods that are usually engaged in the computational/theoretical calculations for the charge distributions calculations in a compound are Mulliken and natural population analysis [55]. However, these two methods have been found to provide at least a qualitative understanding of the structure and reactivity of molecule [56]. Also, they predict quantitatively negative electronic charges for all the heteroatoms, but natural population charges are usually more negative in values [42]. In this present work,

Mulliken population charge analysis is used in analyzing charge population distributions as shown in Table 5. Critical analysis of the charge population distributions shows that the computational methods used predicted quantitatively very similar (but not outright the same) charge distributions for compound A and B (Figure 6). Previous studied has shown that charge distributions respond more to the basis sets rather than the computational methods used for the calculation [57, 58].

Table 5: Mulliken Charges on atoms (let it be in graphs)

	A				B			
Atom	B3LYP/6-311++G(d,p)	wB97xD/6-311++G(d,p)	M06/6-311++G(d,p)	MP2/6-311++G(d,p)	B3LYP/6-311++G(d,p)	wB97xD/6-311++G(d,p)	M06/6-311++G(d,p)	MP2/6-311++G(d,p)
N1	-0.119	-0.171	-0.154	-0.156	-0.027	-0.012	0.035	0.000
O1	-0.288	-0.277	-0.291	-0.244	-0.171	-0.172	-0.197	-0.176
C1	-0.003	-0.022	-0.032	-0.020	-0.240	-0.354	-0.348	-0.344
C2	-0.001	0.007	0.004	-0.020	-0.101	-0.130	-0.126	-0.104
C3	-0.023	-0.008	-0.034	0.022	-0.487	-0.507	-0.534	-0.476
C4	0.186	0.158	0.106	0.178	0.538	0.567	0.485	0.563
C5	0.125	0.106	0.175	0.124	0.246	0.303	0.339	0.303
C6	-0.203	-0.231	-0.217	-0.218	-0.232	-0.265	-0.245	0.259
C7	-0.213	-0.268	-0.239	-0.259	-0.017	-0.076	-0.075	-0.070
C8	-0.442	-0.502	-0.460	-0.494	-0.545	-0.610	-0.570	-0.579
C9	-0.248	-0.284	-0.268	-0.290	-0.219	-0.242	-0.204	-0.252
H2	0.203	0.249	0.255	0.221	0.194	0.235	0.238	0.216
H3	0.303	0.345	0.339	0.322	0.284	0.296	0.309	0.286
H4	0.157	0.197	0.187	0.178	0.159	0.202	0.193	0.182
H5	0.142	0.185	0.173	0.167	0.178	0.223	0.214	0.206
H9	0.164	0.206	0.199	0.185	0.155	0.198	0.193	0.180
H10	0.128	0.146	0.110	0.150	0.174	0.202	0.179	0.191
H14	0.133	0.163	0.140	0.152	0.110	0.143	0.115	0.132

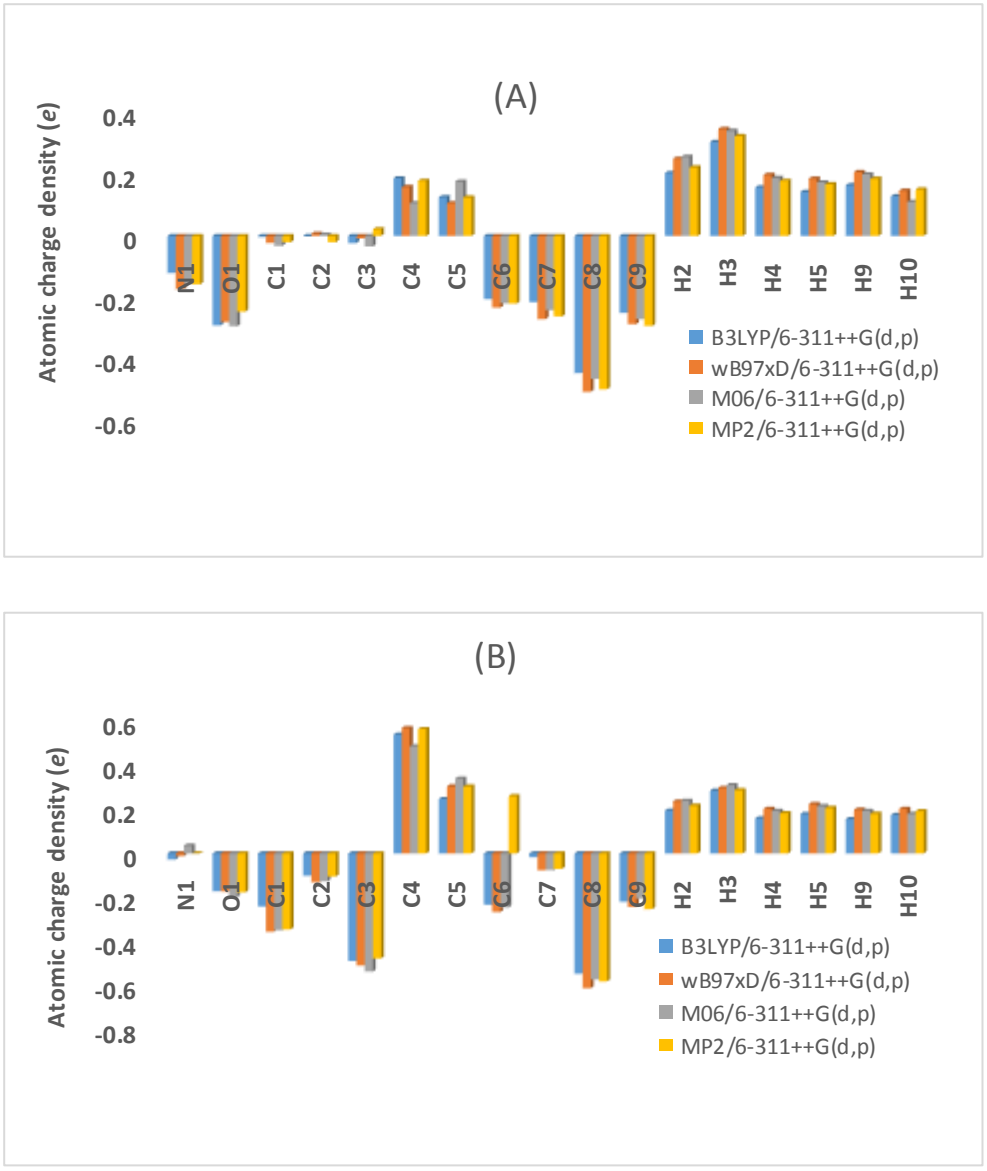

Figure 6: Effect of different quantum chemical methods on atomic charges

4.0 Conclusion

This present work study examined the molecular and electronic properties of 1H-indole-3-carbaldehyde and its enol-tautomer, (Z)-indol-3-ylidenemethanol various quantum chemical methods. The parameters examined includes the E_{HOMO}, E_{LUMO}, band gap, dipole moment, softness (σ), chemical hardness (η), chemical potential (μ), ionization potential (IP), electron affinity (EA) and nucleophilicity index (ω). The molecular properties calculated showed that

compound A would be hard, more stable thermodynamically and less labile than B. The molecular electrostatic potential (MEP) map also revealed that N-H hydrogen and carbonyl oxygen are favourable site for nucleophilic (blue color) and electrophilic (red color) activities for compound A, whereas O-H hydrogen and N of indole are

most feasible site for nucleophilic and electrophilic activities for compound B. The stability and thermodynamics results indicated that compound B can be synthesized. The vibration frequency simulated using computational methods are in agreement with available experimental data for compound A, therefore they can be used to predict properties of similar compounds with reasonably high degree of accuracy.

References

[1] Hidgon JV, Delage BW, Dashwood RH, Pharmacol Res, 2007, 55(3): 224
[2] De Ponti F, Gut, 2004, 53: 1520–1535
[3] Sibel S et al., Il Farmaco. 2000, 55: 246–248
[4] George G et al., Pharmacotherapy, 2005, 25: 1
[5] Suzen S et al., Il Farmaco, 1998, 53: 525–527
[6] Dun-xian T et al., Current Topics in Medicinal Chemistry, 2002, 2: 181-197
[7] Nagata S, Takeyama K, Fukuya F, Nagai R, Hosoki K, Nishimura K, Deguchi T, Karasawa T, Arzneimittel-Forschung/Drug Res, 1995, 45: 853
[8] Vlasova MI, Kogan NA, Lesiovskaya YY, Pastushenkov LV, Khimico-Farmatsevticheskii Zh, 1992, 26: 23
[9] Mugnaini M, Antolini M, Corsi M, Vanamsterdam FT, J Recept Signal Transduct Res, 1998, 18: 91
[10] Kipp C, Young AR, Photochem Photobiol, 1999, 70: 191
[11] Kutschy P, Dzurilla M, Takasugi M, Sabova A, Coll Czech Chem Commun, 1999, 64: 348
[12] Biswal S, Sahoo U, Sethy S, Kumar HKS, Banerjee M, Asian J Pharm Clin Res, 2012, 5(1): 1-6
[13] Mardia TE, Nehal AH, Dalia AO, Khadiga MA, Adv Oncology Res doi: 10.18282/amor.v1.i1.12
[14] Li JJ, Indoles, oxindoles, and azaindoles. In: Li JJ, editor. Heterocyclic chemistry in drug discovery.Hoboken, New Jersey: John wiley and Sons Inc; 2013. pp. 54–118
[15] Suwaiyan A, Zwarich R, Spectrochim Acta A, 1986, 42: 1017
[16] Takeuchi H, Harada I, Spectrochim Acta A, 1986, 42: 1069
[17] Masoud FA, Salimeh A, Marjan E, Marjan D, and Farzad K, Iran J Pharm Res, 2014, 13: 35–42
[18] Chen HS, Kuo SC, Teng CM, Lee FY, Wang JP, Lee YC, Kuo CW, Huang CC, Wu CC, Huang LJ, Bioorg Med Chem 2008, 16: 1262–1278
[19] Ahuja P, Siddiqui N. Eur J of Med Chem, 2014, 80: 509-22
[20] Collier WB, J Chem Phys 1988, 88 7295
[21] Majoube M, Vergoten C, J Raman Spectrosc, 1992, 23: 431
[22] Barstis TLO, Grace LI, Dum TM, Lubman DM, J Phys Chem, 1993, 97: 5820
[23] W.B. Collier, I. Magdó, T.D. Klots, J. Chem. Phys. 1999, 110: 5710
[24] Xue Y, Guo Y, Xu XJ, Xie DQ, Yan GS, Acta Chim Sin, 2000, 58: 1254
[25] Jalbout AF, Hall CS, Adamowicz L, J Chem Phys, 2003, 118: 10541
[25] Yourtsever M, Yurtsever E, Polymer, 2002, 43: 6019

[27] Unterberg C, Jansen A, Gerhads M, J Chem Phys, 2000, 113: 7945
[28] Sundaraganesan N, Umamaheswari H, Dominic JB, Meganathan C, Ramalingam M, J Mol Struct THEOCHEM, 2008, 84: 850
[29] Ferenc B, Paula VP, Ildikó M-Z, Monica T, Hans M, Dan-Florin I, Spectrochimica Acta Part A, 2009, 74: 1031–1045
[30] Becke AD, J Chem Phys, 1993, 98: 5648
[31] Lee C, Yang W, Parr RG, Phys Rev B, 1988, 37: 785
[32] Spartan 14, wavefunction Inc. 18401 Von Karman Avenue, Irvene CA 92612, USA 2014
[33] Zhou Z and Navangul HV, J Phys Org Chem, 1990, 3: 784-788
[34] Koopmans T, Physica, 1934, 1: 104-113
[35] Parr RG, Szentpaly L and Liu S, J Am Chem Soc, 1999, 121:1922-1924
[36] Domingo LR, Aurell M, Contreras M and Perez P, J Phys Chem A, 2002, 106:6871-6876
[37] Dileep CS, Abdoh MMM, Chakravarthy MP, Mohana KN and Sridhar MA, Acta Cryst. 2012, E68, o3135 doi:10.1107/S1600536812040573
[38] Saeed S, Rashid N, Jones PG, Ali M and Hussain R, Europ J Med Chem, 2010, 45: 1323
[39] Masoome SSS, J Phys Theor Chem IAU Iran, 13 (3) 277-288
[40] Adeoye IO and Semire B, IJBAS-IJENS 13(2): 101-107
[41] Silverstein M, Basseler GC and Morill C, Spectrometric Identification of Organic compounds. Wiley, New York, 1981.

[42] Semire B, Mutiu OA, and Oyebamiji AK, Journal of Physical and Theoretical Chemistry, 2017, 13(4): 353-377
[43] Zhang R, Dub B, Sun G and Sun Y, Spectrochim Acta A, 2010, 75(3): 1115-1124
[44] Merrick JP, Moran D and Radom L, J. Phys. Chem. A 2007, 111(45):11683-11700
[45] Sundaragansan N, Elango G, Sebastian S and Subraman P, Indian J Pure Applied Phys, 2009, 47:481-490
[46] Sundaraganesan N, Meganathan C, Anand B., Christine L, Spectrochimica Acta Part A: Molecular and Biomolecular Spectroscopy, 2007, 66(3): 773-780
[47] Siddiqui SA, Dwivedi A, Singh PK, Hasan T, Jain S, Prasad O, Misra N, J Struct Chem, , 2009, 50: 411-420
[48] Premkumar R, Mohamed R, Mathavan A, and Milton FBA. Structural, vibrational spectroscopic and quantum chemical studies on indole-3-carboxaldehyde AIP Conference Proceedings, 2017, 1832, 140041; doi: 10.1063/1.4980823
View online: http://dx.doi.org/10.1063/1.4980823
[49] Barbara M-O, Danuta M, Adam P, Journal of Molecular Structure, 2004, 688: 79–86
[50] Nikoofard H, Sabzyan H, J Fluorine Chem, 2007, 128(6): 668
[51] Semire B, Adejoro IA and Odunola OA, Eclética Química, 2011, 36(3): 26-30

[52] Ravindra MG, Anupam B, Semire B. Bishwajit G and Suresh KJ, Journal of Membrane Science, 2014, 472: 154-166
[53] Semire B and Odunola OA, Quim Nova, 2014, 37(5): 833-838
[54] Fatmah AMA, Asha R, Rajub K, Yohannan PC, Nadia G, Haress AAE, Mahmoud BE, Abdulaziz AA, Christian VA, Javeed AW, Molecular and Biomolecular Spectroscopy, 2015, 136: 520-533
[55] Murrell JN, Kettle SF and Tedder JM, The Chemical Bond, John Wiley & Sons, Chichester, 1985
[56] Grüber C, and Buss V, Chemosphere, 1989, 19: 1595-1609.
[57] Carbó-Dorca R and Bultinck P, Journal of Mathematical Chemistry, 2004, 36: 231-239
[58] Jordan J, Philips MA, Hudspeth PM, Browne Jr.JE, Peralta, Chemical Physics Letters, 2010, 495(1–3): 146-150